2021

# Tri-Molybdenum Phosphide ($Mo_3P$) and Multi-Walled Carbon Nanotube Junctions for Volatile Organic Compounds (VOCs) Detection

Baleeswaraiah Muchharla

Praveen Malali

Brenna Daniel

Alireza Kondori

Mohammad Asadi

*See next page for additional authors*



## Original Publication Citation

Baleeswaraiah, M., Malali, P., Breena, D. ... Kumar, K., Karoui, A., Kumar B. (2021) Tri-molybdenum phosphide ($Mo_3P$) and multi-walled carbon nanotube junctions for volatile organic compounds (VOCs) detection. *Applied Physics Letters*, *119*(11), 1-7, Article 113101. https://doi.org/10.1063/5.0059378

Applied Physics Letters ARTICLE scitation.org/journal/apl

# Tri-molybdenum phosphide ($Mo_3P$) and multi-walled carbon nanotube junctions for volatile organic compounds (VOCs) detection

Cite as: Appl. Phys. Lett. **119**, 113101 (2021); doi: 10.1063/5.0059378
Submitted: 9 June 2021 · Accepted: 5 August 2021 ·
Published Online: 13 September 2021



Baleeswaraiah Muchharla,[1] Praveen Malali,[1] Brenna Daniel,[1] Alireza Kondori,[2] Mohammad Asadi,[2] Wei Cao,[3] Hani E. Elsayed-Ali,[3] Mickaël Castro,[4] Mehran Elahi,[1] Adetayo Adedeji,[1] Kishor Kumar Sadasivuni,[5] Muni Raj Maurya,[5] Kapil Kumar,[6] Abdennaceur Karoui,[7] and Bijandra Kumar[1,a)]

## AFFILIATIONS

[1]Department of Mathematics, Computer Science and Engineering Technology, Elizabeth City State University, Elizabeth City, North Carolina 27909, USA
[2]Department of Chemical and Biological Engineering, Illinois Institute of Technology, Chicago, Illinois 60616, USA
[3]Department of Electrical and Computer Engineering, Old Dominion University, Norfolk, Virginia 23529, USA
[4]Smart Plastics Group, Bretagne Loire University (UBL), IRDL CNRS 6027-UBS, 56622 Lorient, France
[5]Center for Advanced Materials, Qatar University, PO Box, Doha 2713, Qatar
[6]National Institute of Technology Delhi, New Delhi 110040, India
[7]Center for Research Excellence in Science and Technology (CREST), Department of Mathematics and Physics, North Carolina Central University, Durham, North Carolina 27707, USA

[a)]**Author to whom correspondence should be addressed:** BKumar@ecsu.edu. **Tel.:** +1(252) 335-3290. **Fax:** +1(252) 335-3760

## ABSTRACT

Detection and analysis of volatile organic compounds' (VOCs) biomarkers lead to improvement in healthcare diagnosis and other applications such as chemical threat detection and food quality control. Here, we report on tri-molybdenum phosphide ($Mo_3P$) and multi-walled carbon nanotube (MWCNT) junction-based vapor quantum resistive sensors (vQRSs), which exhibit more than one order of magnitude higher sensitivity and superior selectivity for biomarkers in comparison to pristine MWCNT junctions based vQRSs. Transmission electron microscope/scanning tunneling electron microscope with energy dispersive x-ray spectroscopy, x-ray diffraction, and x-ray photoelectron spectroscopy studies reveal the crystallinity and the presence of Mo and P elements in the network. The presence of $Mo_3P$ clearly enhanced the performance of vQRS as evidenced in sensitivity and selectivity studies. The vQRSs are stable over extended periods of time and are reproducible, making them a potential candidate for sensing related applications.



The rapid spread of the novel coronavirus outbreak, which occurred at the end of 2019, has changed the perspective and living style of mankind across the globe. Remote and non-contact diagnosis has become an essential part of medical care. Real-time monitoring of medical conditions will be vital in the healthcare system to detect and diagnose diseases at an early-stage. Detection of volatile organic compounds (VOCs) is a new frontier in the rapid, sensitive, selective, and non-invasive analysis and medical diagnosis of human diseases. VOCs, generated in the human body, could provide reliable and valuable indications of human health. Hundreds of different biologically generated VOC molecules that are released from exhaled breath could serve as biomarkers for early-stage detection of diseases (e.g., cancer).[1–4] For instance, VOCs' profile of exhaled breath, characterized by the use of an electronic nose (e-nose) designed by combining multiple individual sensors together, has attracted immediate attention for the early-stage detection of lung cancer and other diseases (e.g., tuberculosis, diabetes).[5–11] However, e-nose performance is highly dependent on the use of individual sensors assembled in an array.[11–13] The key challenges in designing individual sensors include their unique sensing patterns, high sensitivity, and superior stability with repeatable performance, among others. Different sensing platforms, such as a p–n junction diode,[14] quantum resistive sensors via spraying layer-by-layer (sLbL)[15] or drop-casting,[16] random networks,[17] and field effect transistors (FETs),[18] have been utilized for VOCs' sensing. Vapor

quantum resistive sensors (vQRSs) based on carbon nanotube (CNT) random networks with facile fabrication methodologies have advantages over others due to high rate of reproducibility, easy fabrication methodologies, and simple working principles over FETs and diode-based sensors.[15,17,19]

It should be noted that selectivity, sensitivity, and stability are important figures of merit while characterizing the VOC sensors. In the ideal case, VOC sensors must have a wide selectivity of analytes, high sensitivity for good detection, and should be stable upon exposure to VOCs for an extended period of time under atmospheric pressure at room temperature. Carbon nanotubes (CNTs) are potential candidates as active materials for VOC/gas sensors due to their high surface area and their ability to change electrical properties at room temperature upon exposure to different VOCs/gases.[20–23] Individual CNT-based sensors suffer from poor selectivity and low sensitivity due to the lack of surface functionality, resulting in a poor interaction with analytes. However, creating a CNT junction via the fabrication of the CNT network is the easiest way to originate sites for analyte accumulation and, thus, improve sensitivity and selectivity. These interaction points could be within the nanotubes, leading to an intra-CNT interaction, or interactions among different CNTs leading to inter-CNT interactions, or effects due to contact between the tubes and the metal electrodes. It is unlikely that the intra-CNT interaction is the cause of the change in the charge transport in multi-walled CNTs, as the inner walls can provide a conductive path even when the analyte interacts with the outer walls.[24] In the case of MWCNT vQRSs, inter-CNT interactions and CNT-metal electrode junctions dominate the charge transport behavior when exposed to the analyte gas molecules. The CNT–CNT junctions can be modified to improve the sensitivity and selectivity of the sensor by introducing the host molecule at or within the junctions. In fact, CNT–CNT junctions embedded within polymeric matrices exhibit superior selectivity with a unique VOC sensing pattern.[15,17,19,24–28] Aside from polymeric molecules that degrade with time and, thus, vQRSs performance, metal-based nanostructures (e.g., $SnO_2$) were also deposited on the CNTs surface to further improve the sensitivity of the CNT network, presumably without compromising the stability.[25] Herein, we developed vQRSs based on the modified CNTs and $Mo_3P$ nanoparticle junctions to detect VOCs with improved sensitivity and unique sensing patterns. The $Mo_3P$ nanoparticles were selected due to their different electronic and chemical nature, which was utilized for the hydrogen evolution reaction due to the appropriate binding of the hydrogen ions on the $Mo_3P$ surface. Considering the unique electro-chemical properties of $Mo_3P$ nanoparticles, we believe that the nano-junctions formed between CNTs and adsorbed $Mo_3P$ nanoparticles would exhibit a unique sensing pattern with improved sensitivity. The focus of the present work is to show that $Mo_3P$ nanoparticles and MWCNT junctions could be used for VOC biomarkers detection such as methanol, isopropanol, water, toluene, ethanol, acetone, and chloroform under ambient conditions. These VOCs are selected as they are the key elements present in higher concentrations (e.g., methanol ∼461 ppb, ethanol ∼112 ppb, acetone ∼477 ppb, and isopropanol ∼18 ppb) in everybody's exhaled breath.[29] Another study observed 103 VOCs in exhaled breath of lung cancer patients, and it was reported that the median concentrations of methanol are lower in lung cancer patients (118.5 ppb) than in healthy subjects (142.0 ppb), and median concentrations of acetone are lower in lung cancer patients (458.7 ppb) than in healthy subjects (627.5 ppb). In the same study, it was reported that the appearance of toluene in the exhaled breath was strongly influenced by smoking habits.[30] CNTs-$Mo_3P$ junctions were built by fabrication of $Mo_3P$ and CNTs' co-dispersed solution via the drop casting method on interdigitated electrodes. Transmission electron microscope (TEM)/scanning tunneling electron microscope (STEM) with energy dispersive x-ray spectroscopy (EDS) imaging was used to visualize the morphology of the conducting network of fabricated sensors. Our results indicated $Mo_3P$-MWCNTs' vQRS displayed high sensitivity, selectivity, and stability displayed at room temperature clearly demonstrate the good potential in the detection of VOCs, which could be a promising candidate in healthcare diagnosis, for instance, early detection of lung cancer. The sensing experiments suggest significantly enhanced sensitivity (in the order of ∼7–42 times higher than pristine CNTs) of the developed sensors with a unique discrimination ability.

Multi-walled carbon nanotubes (MWCNTs, outer diameter: 20–30 nm, inside diameter: 5–10 nm, ash: <1.5 wt. %, purity: >95 wt. %, length: 10–30 $\mu$m, specific surface area: 110 $m^2/g$, electrical conductivity: >100 S/cm, bulk density: 0.28 $g/cm^3$, and true density: ∼2.1 $g/cm^3$) were purchased from Cheap Tubes, Inc. (Brattleboro, Vermont) and used without any further purification process. Tri-molybdenum phosphide ($Mo_3P$) nanoparticles were synthesized using a colloidal chemistry technique followed by the two-steps thermal sintering method.[31–33] Ammonium molybdate tetrahydrate [$(NH_4)_6Mo_7O_{24}{\cdot}4H_2O$, Sigma-Aldrich, Bioultra, > 99.0%], diammonium phosphate dibasic [$(NH_4)_2HPO_4$, Sigma-Aldrich, ACS reagent, >98.0%], and citric acid ($C_6H_8O_7$, Sigma-Aldrich, ACS reagent, >99.5%) were used in molar ratios of 1:3:6, respectively. First, ammonium molybdate tetrahydrate and diammonium phosphate dibasic were mixed in sufficient amount of DI water in a flat-bottom flask. A hotplate magnetic stirrer was used to dissolve the powders in DI water. Once the powder was completely dissolved, citric acid was added to the solution. Thereafter, the solution was heated up to 90 °C and held at 90 °C overnight. The final milky-white solution was then cooled down to the room temperature for few more hours until the reaction products precipitate. The excess DI water was extracted from the flask using a pipette, and the precipitates were transferred and held in an oven at a temperature of 120 °C to completely dry out the water contents. Next, an agate mortar and a pestle were used to grind the dried precipitates into a fine white powder. The powder was then transferred into an alumina crucible and moved into a dual-zone tubular furnace for further heat treatments. First, temperatures were ramped (i) from 25 to 500 °C over 60 min with a dwell time of 6 h under a controlled flow of nitrogen ($N_2$) and (ii) from 500 to 850 °C over 60 min with a dwell time of 2 h under a controlled flow of hydrogen–argon (8%$H_2$/Ar). The sample was then cooled down to the room temperature.

$Mo_3P$ and MWCNT solutions were prepared via sonication methods. MWCNTs (2 mg) were dispersed in methanol at a concentration of 0.2 mg/ml, using ultra-sonication (40 kHz, 120 V) bath for 30 min under controlled condition (temperature −25 °C). $Mo_3P$ nanoparticles, synthesized by a colloidal chemistry technique followed by the two-steps thermal sintering method, were dispersed in methanol at a concentration of 0.2 mg/ml using ultra-sonication. The sensors were fabricated using commercially available inter-digitated electrodes by drop-casting 10 $\mu$l $Mo_3P$, and MWCNT solutions were carefully deposited on the electrodes and the samples were then dried overnight in ambient condition. The fabricated vQRSs were exposed to saturated

VOCs in the dynamic-mode with 100 sccm flow rate, which contained 50% of $N_2$ gas and 50% of saturated analyte vapors using an indigenously build sensing device. A schematic diagram depicting the experimental setup is provided in the supplementary material (Fig. S2). The sensitivity of the sensors was analyzed by measuring the changes in the electrical current/resistance upon exposure to alternate cycles (5 min) of dry $N_2$ and pure analyte vapor. The current vs time (i–t) signals were recorded using the potentiostat by applying 100 mV constant potential between source and drain terminals of the sensor. It should be noted that the testing experiments have been conducted at atmospheric pressure, at 25 °C, and with the relative humidity (RH) levels of 40%, to mimic realistic application conditions of the sensor. The relative amplitude is obtained by taking % change of resistance according to

$$A_r = \frac{(R - R_0)}{R_0} * 100\%, \quad (1)$$

where $R_0$ is the initial resistance of sensors under $N_2$ gas flow and R is the resistance in the presence of VOCs. Furthermore, to remove the ambiguity of the number of molecules being different for saturated vapor pressure of each analyte and improve the accuracy, the relative amplitude is normalized with the number of analyte molecules and the normalized relative amplitude ($N–A_r$) is calculated using Eq. (1)

$$N - A_r = \frac{A_r}{[VOC]_{sat}^{T,P}} \times 10^5, \quad (2)$$

where $[VOC]_{sat}^{T,P}$ is the concentration of vapor in saturated conditions calculated by ANTOINE's equation.[34] The seven VOCs (methanol, ethanol, chloroform, acetone, toluene, isopropanol, and water) were selected consisting diverse chemical (e.g., chemical nature) and physical properties (e.g., polarity, atomic sizes, dipole moments) as provided in the supplementary material (Tables S1 and S2).[17,19,35] Here, it should be noted that all reported sensing curves represent measured data without any treatment such as baseline correction or alignment of the gas switching. They have been collected by performing experiments in realistic environmental conditions (environmental temperature, pressure, and humidity).

TEM/STEM with EDS analysis evidence the formation of a random conducting network of $Mo_3P$-MWCNTs [Figs. 1(a)–1(c)]. The morphology of $Mo_3P$-MWCNT network displays physical adsorption of $Mo_3P$ nanoparticles onto the surface of MWCNTs, and thus creating $Mo_3P$-MWCNT junctions [Fig. 1(a)]. A small amount of cobalt was also observed, which could be appeared due to metal catalyst impurity during MWCNT growth. Individual elements mapped as Mo [Fig. 1(b)] and P [Fig. 1(c)] further confirm the presence of $Mo_3P$ nanoparticles on MWCNTs. Extended EDS spectrum further confirms the absence of other impurities (except Co), which is displayed in Fig. S1. Used $Mo_3P$ nanoparticles were also analyzed using characterization techniques such as x-ray diffraction (XRD) and x-ray photoelectron spectroscopy (XPS). The XRD results shown in Fig. 1(d) are obtained by a Bruker D2 PHASER diffractometer Bragg–Brentano geometry employing Ni filtered Cu $K_\alpha$ radiation. Diffraction patterns

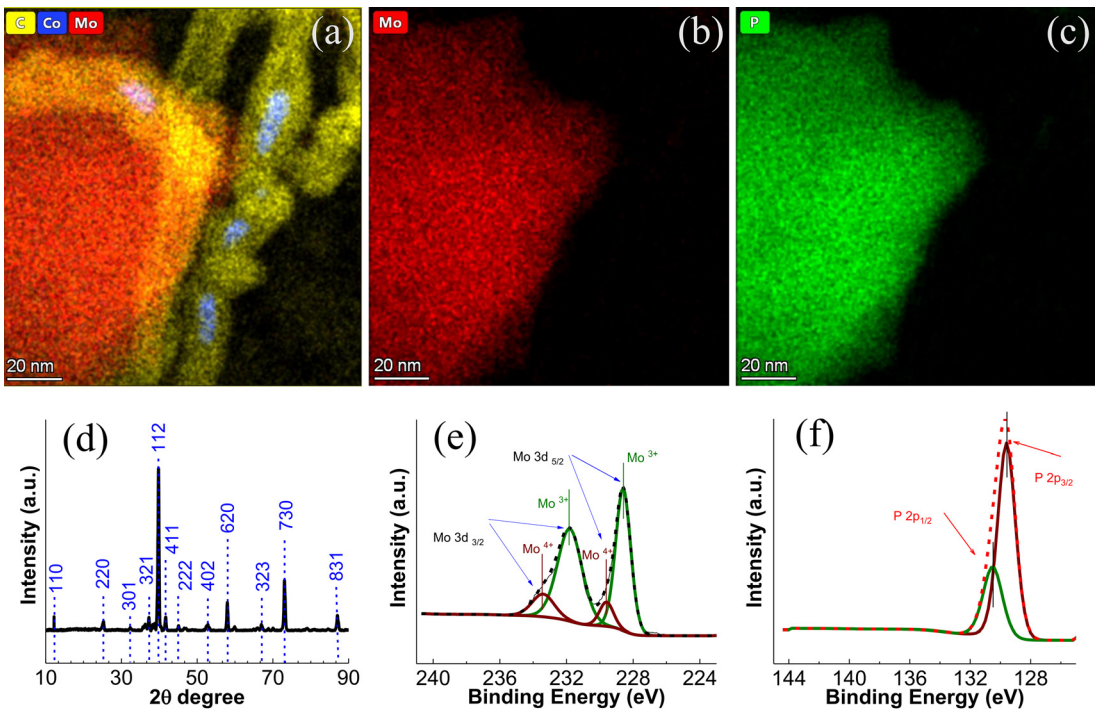


**FIG. 1.** Structural and morphological characterization of the $Mo_3P$-MWCNT samples performed by TEM/STEM techniques equipped with EDS: (a) elemental mapping of $Mo_3P$-MWCNTs indicating a junction between $Mo_3P$ and MWCNTs, (b) Mo element mapping, (c) P element mapping, (d) XRD pattern, and (e) and (f) XPS spectrum of the $Mo_3P$ sample.

were collected from 0 to 100° $2\theta$° with a step width of 0.2 and a counting time of 1s/step. All other parameters were chosen to enhance the signal to noise in the spectra. Figure 1(d) shows the XRD peaks of the $Mo_3P$ sample corresponding to a tetragonal system with SPGR of I $\bar{4}$2m that also matches with ICDD (04–004-3005) database, confirming its crystalline structure with an average crystallite size of 20 nm, which is estimated using the Scherrer equation [$d = \frac{K\lambda}{\beta \cos\theta}$, where K = 0.98 for spheres (dimensionless), the x-ray wavelength of $\lambda = 0.158$ nm for the Cu x-ray tube, $\beta$ is the line broadening at half of the maximum intensity in radians, and $\theta$ is the Bragg angle in radians].[36–39] Figures 1(e) and 1(f) show the XPS spectra of the Mo 3d and P 2p of $Mo_3P$ obtained by a Thermo-Scientific ESCALAB 250Xi instrument. All the spectra are calibrated to the C 1s C–C bond binding energy at 284.8 eV. Figure 1(e) shows the Mo 3d XPS spectrum with peaks at 228.6, 229.6, 231.8, and 233.4 eV, confirming the presence of standard $Mo^{3+}$ and $Mo^{4+}$, where the XPS spectrum of P 2p shown in Fig. 1(f) indicates doublet peaks at 129.6 and 130.4 eV that are attributed to the low valence of P.[31,32]

Figure 2 displays the normalized relative amplitude (N–$A_r$) vs time of MWCNTs and $Mo_3P$-MWCNT vQRSs exposed to all examined VOCs. As expected, an increase in the N–$A_r$ magnitude has been observed when the sensors were subjected to the VOCs flow, followed by a return to the initial value, when the sensors were swept by the inert carrier gas ($N_2$). For all seven VOCs, $Mo_3P$-MWCNT vQRSs exhibit significantly higher sensitivity in comparison to the MWCNTs based vQRSs. In the case of methanol, $Mo_3P$-MWCNT sensors show ~12 times higher sensitivity than that of MWCNT vQRSs [Fig. 2(a)]. Similarly, ~16, ~12, ~7, ~15, ~42, and ~10 times higher sensitivities were observed for methanol, ethanol, isopropanol acetone, chloroform, toluene, and water, respectively (Fig. 2). With the exception of acetone and water molecules, we did not observe any drift in the vQRS baseline, indicating superior sensor reversibility for the VOCs examined. This can be attributed to the complete desorption of the analytes during $N_2$ cycles. In the case of acetone and water, the observed baseline behavior can be explained based on the non-reversible sorption–adsorption phenomenon within the vapor and $N_2$ exposure duration. A comparison N–$A_r$ magnitude of MWCNTs and $Mo_3P$-MWCNT vQRSs exposed to all examined VOCs is provided in the supplementary material (Fig. S3).

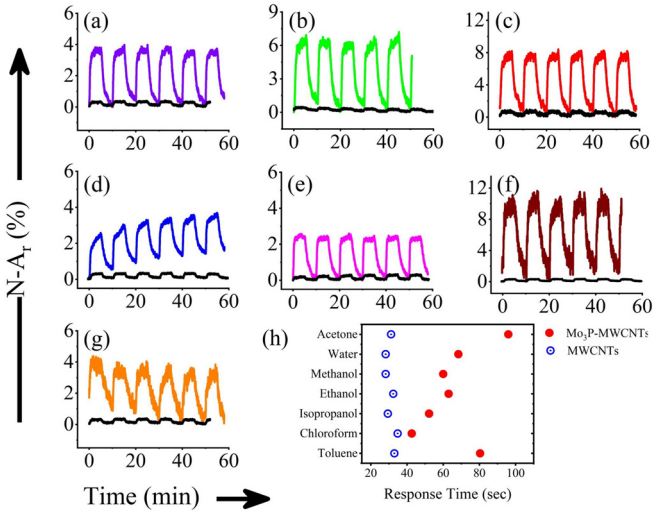


**FIG. 2.** VOCs sensing characterization of fabricated sensors: normalized relative amplitude vs time response of pristine MWCNT (black response) and $Mo_3P$-MWCNT (colored response) sensors (a) methanol, (b) ethanol, (c) isopropanol, (d) acetone, (e) chloroform, (f) toluene, and (g) water vapor. (h) Response time of pristine MWCNT and $Mo_3P$-MWCNT sensors upon exposure to the VOCs.

The response of vQRSs was quick upon exposure to VOCs and was reversible upon switching off the analyte vapor flow in the chamber and purging with $N_2$ gas. The observed response times are on the order of seconds, which is better than colorimetric[40] or metal oxide sensors,[41] which have response times on the order of minutes. The response time is obtained from the sensing behavior, as the time taken to reach 90% of the maximum amplitude upon exposure to the VOCs is displayed in Fig. 2(h). Response time calculations from the sensing behavior are provided in the supplementary material (Fig. S4). The response time varies significantly for the studied VOCs. In the case of sensing via the $Mo_3P$-MWCNT fabricated sensor, compared to the other analytes, chloroform apprehended the shortest response time (~42 s, whereas MWCNTs displayed shorter response times for all analytes compared to the $Mo_3P$-MWCNT sensor. This indicates that $Mo_3P$ is the "limiting/slow" element in the detection mechanism of $Mo_3P$-MWCNT sensors, and that it completely masks the intrinsic sensitivity of the tubes. The recovery time, which is taken as the time for decay to 90% of the signal from the final amplitude upon turning off the VOC exposure, was extracted and results were displayed in the supplementary material (Fig. S5). Similar to response time, the MWCNT sensor recovered quickly than the $Mo_3P$-MWCNT sensor. Figure S6 displays N–$A_r$ vs concentration of analytes gas for several VOCs. Sensitivity of vQRS is increased with the increase in the concentration of analyte gas molecules. For instance, the normalized relative amplitude increased from 2% to 12% when toluene concentration increased from 10% to 50%.

A sensor's network stability is the ability of a sensor to provide reproducible results for a certain period without deviating from the original performance. Figure 3(a) shows that the normalized response amplitude of the sensor is stable under continuous exposure to toluene for 5 h. The vQRS maintained amplitude stable for extended time, implying good stability for the network build of the $Mo_3P$-MWCNT junction in the designed sensor. Sensing response of the $Mo_3P$-MWCNT sensor upon toluene ON/OFF exposure for 5 h is displayed in Fig. S7. The response and recovery of the sensor was quite stable in the studied period. It should be noted here that the signal remained the same for the stability test when exposed to other VOCs. Figure 3(b) displays the current–voltage (I–V) curve of the sensor before and after exposure to toluene for 5 h. The equal slope indicates that conducting properties of the sensor were not altered by exposure to toluene over 5 h, showing the strong stability of the $Mo_3P$-MWCNT junctions. Figure 3(c) shows the electrochemical impedance spectroscopy (EIS) results of the sensor before exposure and after exposure to the analyte gas. The overlapping of both curves in the EIS spectra further confirms that the $Mo_3P$-MWCNT network structure and properties remain identical before and after the long-term exposure.

$Mo_3P$-MWCNT sensors have shown wide range of selectivity, exhibiting the highest response to toluene among the analytes studied. The normalized relative amplitude (right y-axis), plotted for studied analytes is shown in Fig. 4(a), displays the response pattern of sensors

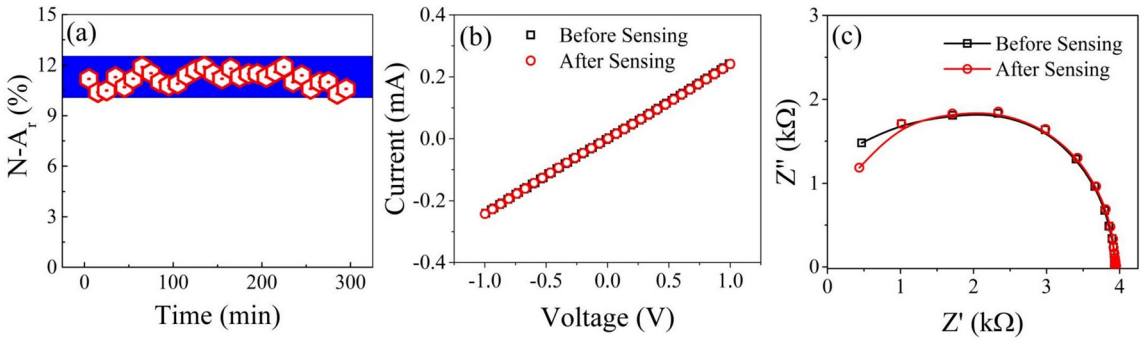


**FIG. 3.** (a) Normalized relative amplitude vs time response of the $Mo_3P$-MWCNT sensor for 5 h displays good stability. (b) I–V characteristics and (c) EIS spectra of the $Mo_3P$-MWCNT sensor before and after performing measurement (a).

exposed to different VOC molecules. The error bars represent the standard deviation of the mean values. We have analyzed our results in light of intrinsic properties (e.g., dipole moment, dielectric constant, polarizability, bond character, surface tension, vapor pressure, solubility parameters, and size), which are provided in the supplementary material (Tables S1 and S2) of the selected VOCs. It is observed that $Mo_3P$ modified CNT junctions or $Mo_3P$-MWCNT junctions led to a sensor with a high inclination toward nonpolar VOC like toluene, as shown in Fig. 4(a). The sensing responses of $Mo_3P$-MWCNT vQRSs can be ascribed to dipole moment. Among the studied solvents, toluene has the lowest dipole moment of about 0.43 D, which exhibited highest N–$A_r$ of about 12%, whereas acetone has the highest dipole moment of about 2.85 D, but it displayed only 2.5% N–$A_r$. Upon exposure of the sensor to the different VOCs, the rate of charge transfer varies based on the electronic structure of VOC, and this electronic structure determines the dipole nature of the VOC. Toluene, which has the lowest dipole moment, disrupts charge transport pathways, resulting in high resistance for the conduction carriers. The sensing response displayed a decreasing behavior with increasing solvent dipole moment as shown in Fig. 4(a). Adsorbed analyte gas (VOC) has impact on the charge transport properties of CNT–CNT junctions. The electronic structure of VOCs with low dipole moment has significant effect on charge conducting pathways, which, in turn, increased resistance resulting in high sensing response, whereas VOC with high dipole moment has less influence on the charge transport within the CNT network of the sensor device resulting in low sensing response. It has been reported that the dipole moment plays a crucial role in dictating the charge transport properties of junctions with the structure Ag/organic functional group/$Ga_2O_3$/EGaIn.[42] Molecular dipoles from simple organic functional groups were introduced into between the Ag and $Ga_2O_3$/EGaIn electrodes and impacted the tunneling junctions, thus altering the rectification of tunneling current.[42] Based on this hypothesis, when dipoles (polar) aligned with the external field produce more current resulting in less sensor response, whereas nonpolar analytes with less diploe moment obstruct the current flow increasing resistance, which, in turn, increases sensor response. This could be a possible reason for our $Mo_3P$-MWCNT vQRS produces high sensing response for nonpolar analytes. Our hypothesis is also

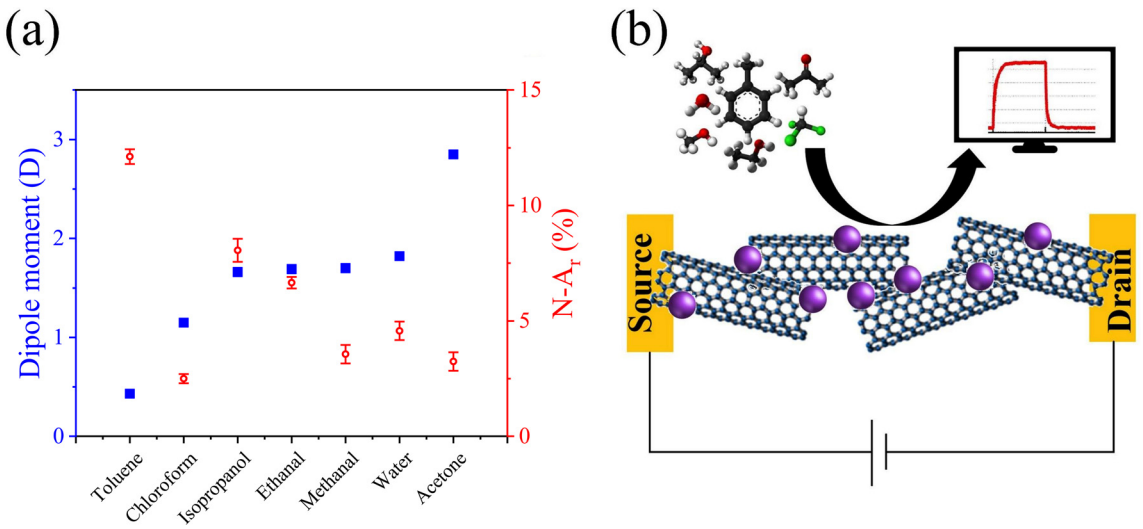


**FIG. 4.** (a) Normalized relative amplitude and dipole moment comparison of VOCs and (b) schematic diagram of $Mo_3P$-MWCNT sensors.

supported by another study, where the ligand capped platinum nanoparticle sensor showed the highest response upon exposure to nonpolar analytes with very low dipole moment (hexane, octane, and decane) and low response to the polar analytes with high dipole moment (ethanol, water) of the same concentration.[43] However, chloroform, with borderline polarity, did not follow the trend for which the dipole moment is about 1.15 D, which is intermediate among the selected VOCs and displayed the lowest N–$A_r$ about 2.5%. A schematic displayed in Fig. 4(b) shows a hypothetical picture of sensors, where $Mo_3P$ nanoparticles adsorbed on to the CNTs interact with the exposed analytes influence the charge transport properties of MWCNTs, resulting responses in the electrical signal. Considering the high sensitivity, selectivity, and stability displayed at room temperature, our vQRS device clearly demonstrates the good potential in the detection of VOCs, which could be a promising candidate in healthcare diagnosis, for instance, early detection of lung cancer. Breath analysis is a promising technique for lung cancer screening. Early detection of lung cancer through analysis of VOC biomarkers in exhaled breath would improve prognosis and enlarge treatment options. Analysis of exhaled breath would be an ideal diagnostic method, since it is non-invasive and totally painless.[44,45]

In summary, we have shown that the $Mo_3P$ modified MWCNT junction in the random network improves the selectivity and sensitivity of the MWCNT vQRS. Morphological studies by SEM and high-resolution TEM images reveal that physiosorbed $Mo_3P$ nanoparticles tend to reside at the CNT–CNT junctions, impacting the electronic transport behavior of the conductive network within the source and drain electrodes. The chemi-resistive behavior of the $Mo_3P$-MWCNT vQRS exhibits significantly improved sensitivity for several analyte gas molecules. The $Mo_3P$-MWCNT vQRS displayed better sensing ability for a nonpolar solvent, e.g., toluene and at the same time, increasing sensitivity was observed for solvents with decreasing dipole moment. $Mo_3P$-MWCNT vQRS displayed great stability and reproducibility upon exposure to the analyte gas molecules for the extended period, although response time of $Mo_3P$-MWCNT vQRS is slow compared to the MWCNT device but selectivity for certain analytes has enhanced remarkably with $Mo_3P$ modification to the MWCNT network. A further study is required to reveal the possible mechanism for the enhanced performance of vQRS for nonpolar solvents. Due to the unique sensing pattern and higher stability, the $Mo_3P$-MWCNTs developed vQRS using facile methodology could be useful in advancing electronic nose applications.

See the supplementary material for TEM/STEM with EDS analysis, the experimental setup schematic, and electrical response data analysis. Physical properties and solubility parameters of VOCs are presented.

All authors have read and approved the final manuscript. Research at the Elizabeth City State University was supported by the National Science Foundation—Major Research Instrument Grant (No. 1920108), Department of National Nuclear Security Administration Grant (No. NA0003979), the Office of Naval Research (No. N00014-17-1-2331), and Qatar National Foundation Grant No. NPRP11S-0110-180247.

## DATA AVAILABILITY

The data that support the findings of this study are available from the corresponding author upon reasonable request.

## REFERENCES

[1]Y. Y. Broza and H. Haick, "Nanomaterial-based sensors for detection of disease by volatile organic compounds," Nanomedicine **8**, 785–806 (2013).
[2]Y. Y. Broza, L. Zuri, and H. Haick, "Combined volatolomics for monitoring of human body chemistry," Sci. Rep. **4**, 4611 (2015).
[3]Y. Y. Broza, P. Mochalski, V. Ruzsanyi, A. Amann, and H. Haick, "Hybrid volatolomics and disease detection," Angew. Chem., Int. Ed. **54**, 11036–11048 (2015).
[4]K. M. Tripathi, T. Kim, D. Losic, and T. T. Tung, "Recent advances in engineered graphene and composites for detection of volatile organic compounds (VOCS) and non-invasive diseases diagnosis," Carbon **110**, 97–129 (2016).
[5]Y. Y. Broza, R. Vishinkin, O. Barash, M. K. Nakhleh, and H. Haick, "Synergy between nanomaterials and volatile organic compounds for non-invasive medical evaluation," Chem. Soc. Rev. **47**, 4781–4859 (2018).
[6]S. Nag, M. Castro, V. Choudhary, and J.-F. Feller, "Sulfonated poly(ether ether ketone) [SPEEK] nanocomposites based on hybrid nanocarbons for the detection and discrimination of some lung cancer VOC biomarkers," J. Mater. Chem. B **5**, 348–359 (2017).
[7]N. Shehada, G. Brönstrup, K. Funka, S. Christiansen, M. Leja, and H. Haick, "Ultrasensitive silicon nanowire for real-world gas sensing: Noninvasive diagnosis of cancer from breath volatolome," Nano Lett. **15**, 1288–1295 (2015).
[8]G. Peng, U. Tisch, O. Adams, M. Hakim, N. Shehada, Y. Y. Broza, S. Billan, R. Abdah-Bortnyak, A. Kuten, and H. Haick, "Diagnosing lung cancer in exhaled breath using gold nanoparticles," Nat. Nanotechnol. **4**, 669–673 (2009).
[9]G. Konvalina and H. Haick, "Sensors for breath testing: From nanomaterials to comprehensive disease detection," Acc. Chem. Res. **47**, 66–76 (2014).
[10]A. T. Güntner, S. Abegg, K. Königstein, P. A. Gerber, A. Schmidt-Trucksäss, and S. E. Pratsinis, "Breath sensors for health monitoring," ACS Sens. **4**, 268–280 (2019).
[11]A. H. Jalal, F. Alam, S. Roychoudhury, Y. Umasankar, N. Pala, and S. Bhansali, "Prospects and challenges of volatile organic compound sensors in human healthcare," ACS Sens. **3**, 1246–1263 (2018).
[12]W. J. Peveler, M. Yazdani, and V. M. Rotello, "Selectivity and specificity: Pros and Cons in sensing," ACS Sens. **1**, 1282–1285 (2016).
[13]T. G. Welearegay, M. F. Diouani, L. Österlund, F. Ionescu, K. Belgacem, H. Smadhi, S. Khaled, A. Kidar, U. Cindemir, D. Laouini, and R. Ionescu, "Ligand-capped ultrapure metal nanoparticle sensors for the detection of cutaneous leishmaniasis disease in exhaled breath," ACS Sens. **3**, 2532–2540 (2018).
[14]S. Dey, S. Nag, S. Santra, S. K. Ray, and P. K. Guha, "Voltage-controlled nio/zno p–n heterojunction diode: A new approach towards selective VOC sensing," Microsyst. Nanoeng. **6**, 35 (2020).
[15]J.-F. Feller, N. Gatt, B. Kumar, and M. Castro, "Selectivity of chemoresistive sensors made of chemically functionalized carbon nanotube random networks for volatile organic compounds (VOC)," Chemosensors **2**, 26–40 (2014).
[16]A. Turner, T. McCoy, W. Cao, A. Karoui, W. M. Maswadeh, B. Vlahovic, H. E. Elsayed-Ali, B. Daniel, M. Castro, K. K. Sadasivuni, M. Elahi, A. Adedeji, and B. Kumar, "Enhanced detection of volatile organic compounds (VOCS) by caffeine modified carbon nanotube junctions," Nano-Struct. Nano-Objects **24**, 100578 (2020).
[17]B. Kumar, M. Castro, and J.-F. Feller, "Tailoring the chemo-resistive response of self-assembled polysaccharide-CNT sensors by chain conformation at tunnel junctions," Carbon **50**, 3627–3634 (2012).
[18]C. Bur, M. Bastuck, D. Puglisi, A. Schütze, A. L. Spetz, and M. Andersson, "Discrimination and quantification of volatile organic compounds in the ppb-range with gas sensitive sic-field effect transistors," in The 28th European Conference on Solid-State Transducers (eUROSENSORS 2014) [Procedia Eng. **87**, 604–607 (2014)].
[19]M. Castro, B. Kumar, J. Feller, Z. Haddi, A. Amari, and B. Bouchikhi, "Novel e-nose for the discrimination of volatile organic biomarkers with an array of carbon nanotubes (CNT) conductive polymer nanocomposites (CPC) sensors," Sens. Actuators, B **159**, 213–219 (2011).

[20]Y. H. Ngo, M. Brothers, J. A. Martin, C. C. Grigsby, K. Fullerton, R. R. Naik, and S. S. Kim, "Chemically enhanced polymer-coated carbon nanotube electronic gas sensor for isopropyl alcohol detection," ACS Omega **3**, 6230–6236 (2018).
[21]W.-T. Koo, Y. Kim, S. Savagatrup, B. Yoon, I. Jeon, S.-J. Choi, I.-D. Kim, and T. M. Swager, "Porous ion exchange polymer matrix for ultrasmall au nanoparticle-decorated carbon nanotube chemiresistors," Chem. Mater. **31**, 5413–5420 (2019).
[22]C. H. Park, V. Schroeder, B. J. Kim, and T. M. Swager, "Ionic liquid-carbon nanotube sensor arrays for human breath related volatile organic compounds," ACS Sens. **3**, 2432–2437 (2018).
[23]S. E. Moulton, A. I. Minett, and G. G. Wallace, "Carbon nanotube based electronic and electrochemical sensors," Sensor Lett. **3**, 183–193 (2005).
[24]V. Schroeder, S. Savagatrup, M. He, S. Lin, and T. M. Swager, "Carbon nanotube chemical sensors," Chem. Rev. **119**, 599–663 (2019).
[25]G. Lu, L. E. Ocola, and J. Chen, "Room-temperature gas sensing based on electron transfer between discrete tin oxide nanocrystals and multiwalled carbon nanotubes," Adv. Mater. **21**, 2487–2491 (2009).
[26]J. Lu, J. Feller, B. Kumar, M. Castro, Y. Kim, Y. Park, and J. Grunlan, "Chemosensitivity of latex-based films containing segregated networks of carbon nanotubes," Sens. Actuators, B **155**, 28–36 (2011).
[27]A. Sachan, M. Castro, V. Choudhary, and J.-F. Feller, "Influence of water molecules on the detection of volatile organic compounds (voc) cancer biomarkers by nanocomposite quantum resistive vapor sensors vqrs," Chemosensors **6**, 64 (2018).
[28]S. Nag, A. Sachan, M. Castro, V. Choudhary, and J. Feller, "Spray layer-by-layer assembly of poss functionalized CNT quantum chemo-resistive sensors with tuneable selectivity and ppm resolution to VOC biomarkers," Sens. Actuators, B **222**, 362–373 (2016).
[29]B. Buszewski, M. Kęsy, T. Ligor, and A. Amann, "Human exhaled air analytics: Biomarkers of diseases," Biomed. Chromatogr. **21**, 553–566 (2007).
[30]A. Bajtarevic, C. Ager, M. Pienz, M. Klieber, K. Schwarz, M. Ligor, T. Ligor, W. Filipiak, H. Denz, M. Fiegl, W. Hilbe, W. Weiss, P. Lukas, H. Jamnig, M. Hackl, A. Haidenberger, B. Buszewski, W. Miekisch, J. Schubert, and A. Amann, "Noninvasive detection of lung cancer by analysis of exhaled breath," BMC Cancer **9**, 348 (2009).
[31]A. Kondori, M. Esmaeilirad, A. Baskin, B. Song, J. Wei, W. Chen, C. U. Segre, R. Shahbazian-Yassar, D. Prendergast, and M. Asadi, "Identifying catalytic active sites of trimolybdenum phosphide ($Mo_3P$) for electrochemical hydrogen evolution," Adv. Energy Mater. **9**, 1900516 (2019).
[32]A. Kondori, Z. Jiang, M. Esmaeilirad, M. Tamadoni Saray, A. Kakekhani, K. Kucuk, P. Navarro Munoz Delgado, S. Maghsoudipour, J. Hayes, C. S. Johnson, C. U. Segre, R. Shahbazian-Yassar, A. M. Rappe, and M. Asadi, "Kinetically stable oxide overlayers on $Mo_3P$ nanoparticles enabling lithium–air batteries with low overpotentials and long cycle life," Adv. Mater. **32**, 2004028 (2020).
[33]P. Xiao, M. A. Sk, L. Thia, X. Ge, R. J. Lim, J.-Y. Wang, K. H. Lim, and X. Wang, "Molybdenum phosphide as an efficient electrocatalyst for the hydrogen evolution reaction," Energy Environ. Sci. **7**, 2624–2629 (2014).
[34]K. Tripathi, A. Sachan, M. Castro, V. Choudhary, S. Sonkar, and J. Feller, "Green carbon nanostructured quantum resistive sensors to detect volatile biomarkers," Sustainable Mater. Technol. **16**, 1–11 (2018).
[35]S. Mao, G. Lu, and J. Chen, "Nanocarbon-based gas sensors: Progress and challenges," J. Mater. Chem. A **2**, 5573–5579 (2014).
[36]U. Holzwarth and N. Gibson, "The Scherrer equation versus the 'Debye-Scherrer equation,'" Nat. Nanotechnol. **6**, 534–534 (2011).
[37]R. Rudman, "Handbook of x-rays, for diffraction, emission, absorption, and microscopy (Kaelble, Emmett F., ed)," J. Chem. Educ. **45**, 443 (1968).
[38]D. Pathak, R. K. Bedi, and D. Kaur, "Growth of $AgInSe_2$ on Si(100) substrate by pulse laser ablation," Surf. Rev. Lett. **16**, 917–923 (2009).
[39]D. Pathak, R. Bedi, and D. Kaur, "Characterization of laser ablated $AgInSe_2$ films," Mater. Sci.-Poland **28**, 199–205 (2010).
[40]M. C. Janzen, J. B. Ponder, D. P. Bailey, C. K. Ingison, and K. S. Suslick, "Colorimetric sensor arrays for volatile organic compounds," Anal. Chem. **78**, 3591–3600 (2006).
[41]F. Paraguay D, M. Miki-Yoshida, J. Morales, J. Solis, and W. Estrada L, "Influence of Al, In, Cu, Fe and Sn dopants on the response of thin film ZnO gas sensor to ethanol vapour," in Proceedings of the 11th International Conference on Thin Films [Thin Solid Films **373**, 137–140 (2000)].
[42]M. Baghbanzadeh, L. Belding, L. Yuan, J. Park, M. H. Al-Sayah, C. M. Bowers, and G. M. Whitesides, "Dipole-induced rectification across $Ag^{TS}/SAM//Ga_2O_3/EGaIn$ junctions," J. Am. Chem. Soc. **141**, 8969–8980 (2019).
[43]E. Dovgolevsky, G. Konvalina, U. Tisch, and H. Haick, "Monolayer-capped cubic platinum nanoparticles for sensing nonpolar analytes in highly humid atmospheres," J. Phys. Chem. C **114**, 14042–14049 (2010).
[44]Z. Jia, A. Patra, V. K. Kutty, and T. Venkatesan, "Critical review of volatile organic compound analysis in breath and in vitro cell culture for detection of lung cancer," Metabolites **9**, 52 (2019).
[45]M. P. C. van der Schee, J. Boschmans, R. Smith, R. Parris, B. Boyle, D. Apthorp, S. Kitchen, R. C. Rintoul, and T. LuCID Consortium, "Early detection of lung cancer through analysis of voc biomarkers in exhaled breath: The lucid study," Eur. Clin. Respir. J. **50**, OA1472 (2017).